Kinetic and Equilibrium Studies of Neutral Red Adsorption onto Spent Ground Coffee from Aqueous Solution

Yingjie Dai*****, Kexin Zhang, Danfeng Zhang and Yanjun Chen
Laboratory of Environmental Remediation, College of Resources and Environment, Northeast Agricultural University, No.59 Mucai Street Xiangfang District, Harbin 150030, China,
dai5188@hotmail.com*

Summary: In this study, the adsorption of neutral red (NR) on the spent ground coffee (SGC) was examined. The effect of various parameters such as pH and adsorbent dose on the removal of NR was investigated. The removal ratios of NR (25 and 40 mg/L) on SGC after 2 h were 95.6 and 90.2%, respectively. The removal ratio of NR is increased by increasing the pH value. Equilibrium data fitted very well in a Langmuir isotherm equation, the adsorption capacity of NR was 136.98 mg/g for SGC. The adsorption mechanisms can be contributed by hydrophobicity interaction at the interface occurs between NR and SGC. The present study shows that the SGC is an inexpensive and easily used NR adsorbent.

Keywords: Spent ground coffee, Thermodynamics, Micropore, Kinetics, Distribution.

Introduction

Some low–cost adsorbents have been tested for removing dyes, such as wheat shells [1], peanut hull [2], hazelnut shells [3], coffee husks [4], banana peel and orange peel [5], cotton waste [6] and olive pomace [7]. However, most of adsorbents are still under development. The amount of spent ground coffee (SGC) was approximately 4.0 million tons in 2011 all over the world [8]. Part of coffee grounds is used as compost, fuel source and animal feed, most of them are burned as waste. Franca *et al.* [9] studied the adsorption behavior of methylene blue by spent coffee grains, and indicated that experimental saturated adsorption amount and the adsorption equilibrium constant for methylene blue were 18.73 mg/g and 0.2687 L/mg, respectively. The experimental data indicate that spent coffee grains are suitable to treat methylene blue dye as adsorbents. The removal of a neutral red (NR) (Table-1) by SGC as an adsorbent has not been reported. The objective of this study was to investigate the adsorption mechanisms for the removal of NR onto SGC. The influences of contact time, pH, and adsorbent dose were analyzed. In addition, the adsorption kinetics, isotherms and thermodynamics of NR onto SGC were investigated.
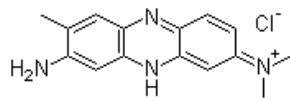
Experimental

Materials

The adsorbent SGC in our study was obtained from Starbucks Corporation, where SGC was produced from coffee beans in China. SGC was washed by deionized water extensively before drying and storage. NR was supplied by Guangfu Institute of Fine Chemical Industry, Tianjin, China. A stock solution (500 mg/L) was prepared by dissolving NR in deionized water; desired concentrations were obtained when needed by diluting the stock solution with deionized water. All chemicals used in our study were of analytical grade, which solutions were being prepared using deionized and distilled water. To adjust the pH, HCl (0.1M) and NaOH (0.1M) solutions were used.

Table-1: Chemical structure and properties of Neutral Red

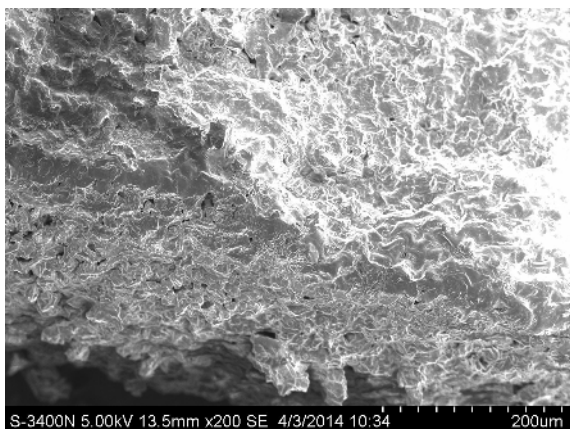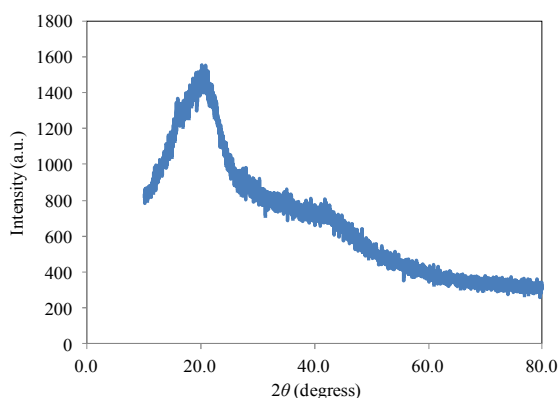| Chemical structure and properties	
CAS Number	553-24-2
Chemical structure	
Chemical formula	$C_{15}H_{16}N_4HCl$
Molar mass	288.78 g/moL
Ionization constant (pK_a)	7.4
λmax	530 nm

Fig. 1: SEM images of the SGC.

Fig. 2: XRD patterns of SGC.

SGC Physic-Chemical Properties

The surfaces properties of SGC were observed using a Scanning Electron Microscope (SEM), S–3400N (Hitachi Ltd. Tokyo, Japan) as shown in Fig. 1. The image of SEM indicates an irregular porous and convex structure. However, there is a relatively small pore structure on the SGC's surface. The study of X−ray diffraction (XRD) was performed by an X−ray Diffractometer 1730 (Philips Ltd. Amsterdam, Netherlands) using Cu Kα radiation. Patterns were recorded from 10° to 80° 2θ at a scan rate 1°/min. The XRD pattern for SGC is shown in Fig. 2. The peak at 20.2° could be assigned to native cellulose or hemicelluloses and their corresponding compounds identified in the JCPDF crystallographic data base [10].

The BET surface area and pore distribution of SGC were measured using a surface analyzer AUTOSORB 6AG (Yuasa Ionics Co., Osaka, Japan). The BET surface areas and the micropore surface areas were evaluated using the *t*–plot method based on N_2 adsorption isotherms [11]. The surface areas of mesopores and macropores were calculated using subtracting the micropore surface areas from the BET surface area. The total pore volume was calculated using Density Functional Theory (DFT) based on the N_2 adsorption isotherms [12]. The numbers of acidic functional groups and basic sites on the surface of SGC were determined using the method developed by Boehm [13]. Acidity was determined using mixing 0.6 g of SGC with 15 mL of $NaHCO_3$ (0.1 M), Na_2CO_3 (0.05 M) or NaOH (0.1 M) solution in a flask. The mixture was then shaken for 48 h at 25 °C and 165 rpm. An aliquot of the solution for each sample was back titrated with HCl (0.1 M). The $NaHCO_3$ neutralizes only the carboxylic groups on the carbon surface, simultaneously, the Na_2CO_3 does the carboxylic and lactonic, and NaOH reacts with the carboxylic, lactonic and phenolic groups. Accordingly, the difference between the groups neutralized by $NaHCO_3$ and Na_2CO_3 are lactones, whereas the difference between those neutralized by Na_2CO_3 and NaOH are the phenolic groups. The same procedure was carried out for the mixtures of 0.5 g of the SGC and 15 mL of HCl (0.1 M) solution to determine the basic sites of the sample surface. The remaining HCl solution was titrated with NaOH (0.1 M) after neutralization. The point of zero charge (pH_{PZC}) for the SGC was determined using the pH drift method [14]. 0.01 M NaCl solutions were aliquoted (50 mL) into a series of flasks. The initial pH (pH_i) was adjusted from 1.98 to 13.25 by the addition of 0.1 M NaOH or HCl. 0.1 g sample of SGC was added to each flask, followed by agitation for 48 h. Then, the final pH (pH_f) of the mixtures was measured. The pH_{pzc} was defined as the point at which the curve determined by $pH_f - pH_i$ crossed the axis $pH_i = pH_f$.

Adsorption Experiment Process

The adsorption features of the adsorbent (SGC) were investigated as a function of contact time, and initial pH. The

adsorption equilibrium and kinetics were obtained from batch experiments, using 100 mL flasks with 25 mL NR solutions. After shaking the flasks for predetermined time intervals, the mixture was filtered, and then the NR concentration in the filtrate was determined using an ultraviolet visible spectrophotometer V–550 (Jasco Co., Tokyo, Japan) at 530 nm. Three replicate were carried out for each experimental treatment. The NR amounts on the adsorbents were calculated from difference between the initial and the equilibrium NR concentrations in the solution. The removal ratio was calculated from dividing the amount of NR adsorbed on SGC by the initial amount of NR in the solution.

Adsorption Kinetics

The controlling mechanism of the adsorption process was investigated using two kinetic models; which were pseudo–first–order and pseudo–second–order models, respectively. The kinetic rate equations can be written as follow,

$$\frac{dq_t}{dt} = [(q]_e - q_t)^n \tag{1}$$

where, q_e and q_t correspond to the amount of NR adsorbed per unit mass of adsorbent (mg/g) at equilibrium and at time t, respectively. k_n is the rate constant for nth order adsorption (k_n units are 1/min for n=1 and g/mg min for n=2). The linearized integrated forms of the equations are shown as follow,

First–order kinetics (n=1):

$$Ln(q_e - q_t) = Ln q_e - k_1 t \tag{2}$$

Second–order kinetics (n=2):

$$\frac{t}{q_t} = \frac{1}{k_2 q_e^2} + \frac{t}{q_e} \tag{3}$$

The straight–line plots of $Ln(q_e - q_t)$ against t and of t/q_t against t were used to determine the rate constants and correlation coefficients (R^2) for the first and second–order kinetic models, respectively. The fitting

equation was selected based on both linear regression R^2 and the calculated q_e values.

Results and Discussion

SGC Physic-Chemical Properties

The acidic and basic functional groups were measured, and data of the surface area are shown in Table-2. The amounts of acidic and basic functional groups on the SGC were 1.49 and 1.24 mmol/g, respectively. The total BET surface area of SGC was 422 m²/g. The surface area of the micropore on SCG was 273 m²/g and was 65% of the total BET surface area of SGC. It indicated that the micropore on SCG play a important role in the press of adsorption. The pH_{PZC} value of SGC was 5.6. The surface charge of SGC is depending on the pH of the solution (Fig. 3).

Table-2: Physical and chemical properties of SGC

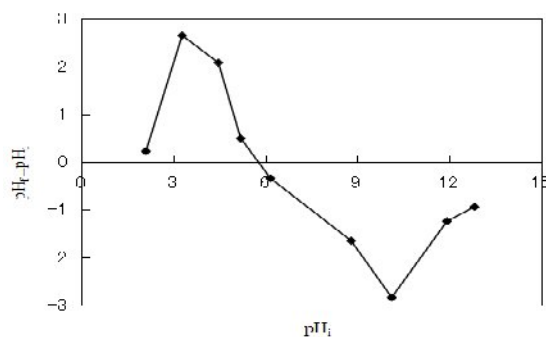| Physical and chemical properties	
Acidic functional groups (mmol/g)	1.49
carboxylic groups(–COOH)	0.45
lactonic groups(–COO⁻)	0.28
phenolic groups (–OH)	0.76
Basic functional groups (mmol/g)	1.24
Surface area (m²/g)	
total (BET surface area)	422
micropore (t-plot)	273
meso & macropore (t-plot)	149
Total pore volume (cm³/g)	0.26
Bulk density(g/cm³)	0.30
Ash (%)	1.54

Fig. 3：   The pH_{PZC} value of SGC.

Adsorption Kinetics

25 mL mixtures of NR (25 and 40 mg/L) and SGC (10 mg) were shaken at 165 rpm. Fig. 4 shows the removal ratios of NR (25 and 40 mg/L) on SGC after 2 h were 95.6 and 90.2%,

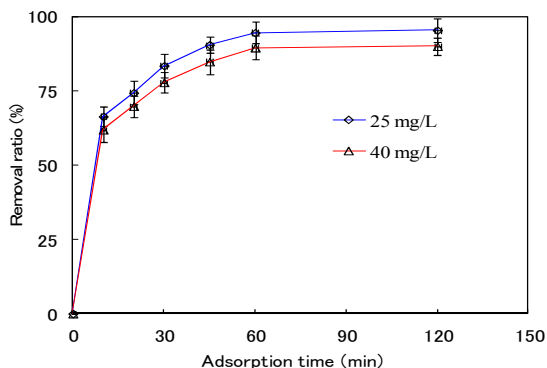respectively. The removal ratio of NR on SGC was increased with adsorption time, and was the highest after 2h.

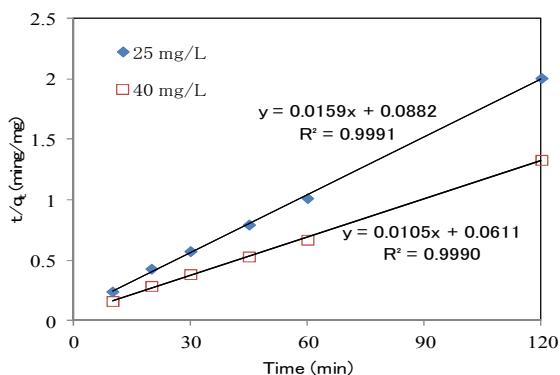Fig. 4**:** Effect of adsorption time on NR adsorption on the SGC.

Fig. 5**:** Pseudo–second–order kinetic plots of NR on SGC.

The controlling mechanism of NR adsorption by SGC was investigated using experimental data into first and second–order fitting models. The results of pseudo–second–order kinetic plots are displayed in Fig 5. The parameter in equation (2) and (3) determined from kinetic constants of NR on SGC are summarized in Table-3. The pseudo–first–order model data do not fall on straight lines. Besides, the calculated q_e values determined from the models differ substantially from those determined experimentally, which suggesting that the studied adsorption of NR on SGC is not a pseudo–first–order reaction. In addition, the R^2 of the pseudo–second–order kinetic model are nearly equal to 1 (Table 3),

and the calculated q_e values (62.89 mg/g for 25 mg/L and 95.23 mg/g for 40 mg/L) are acceptable compared with the experimental data (59.75 mg/g for 25 mg/L and 90.20 mg/g for 40 mg/L). Thus, this suggests that the adsorption of NR on SGC seems to be more of a pseudo–second–order.

Table-3: Kinetic constants of NR on SGC at 25 °C

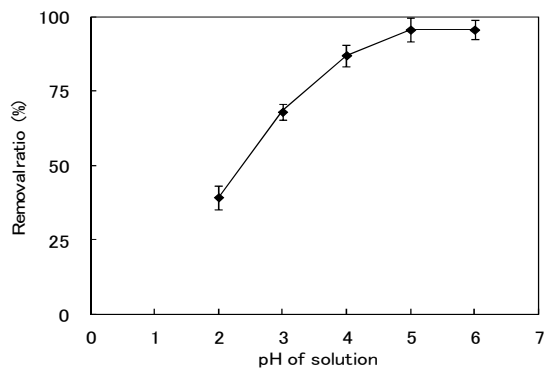|	k_1 (1/min)	Calculated q_e (mg/g)	R^2	Experience q_e (mg/g)
Pseudo-first-order model				
25 mg/L	0.0693	28.78	0.9514	59.75
40 mg/L	0.0774	46.33	0.9083	90.20
Pseudo-second-order model	k_2 (g/mg min)			
25 mg/L	0.0029	62.89	0.9991	59.75
40 mg/L	0.0018	95.23	0.9990	90.20

Fig. 6**:** Effect of pH for NR adsorption on the SGC (C_o =25 mg/L, adsorbent dose=0.4 g/L, at pH 5.0 and 25 °C).

Initial pH Affect NR Removal Ratio

As elucidated in Fig. 6, the NR removal ratios were increased with the increasing pH in the solution. At pH 2.0, the removal ratio of NR was 39.3 %, whereas the removal ratio of NB was 95.6 % at pH 5.0 and 6.0.Then, the pH 5.0 was sit for the following experiments.

NR Removal Affect by Adsorbent Dose

The influence of adsorbent dose on NR adsorption by SGC are shown in Fig. 6. The removal ratio of NR increased and the amount of NR adsorbed decreased with increasing adsorbent dose. The percentages of NR adsorbed increased from 90.2 % to 99.2 % on

SGC, however, the amount of NR adsorbed decreases from 90.2mg/g to 12.4 mg/g with increasing adsorbent dose of SGC from 0.4 g/ L to 3.2 g/ L. Based on the results presented in Fig. 7, the remaining experiments were conducted at an adsorbent dose of 0.4 g/L for SGC.
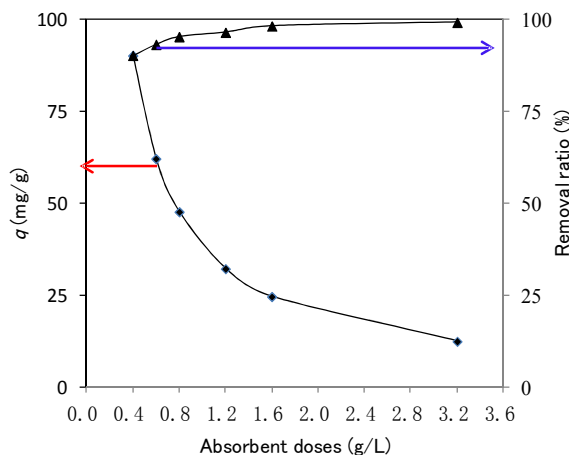

Fig. 7**:**　Effect of adsorbent dose for NR adsorption on the SGC.

Adsorption Isotherm

Langmuir and Freundlich isotherm models were commonly used to analyze the isotherm data. The relationship between the reciprocal of the amount of NR adsorbed on SGC and the reciprocal of the equilibrium concentration of NR in the solution. The parameters in equation (4) and (5), determined from the adsorption isotherms of SGC are summarized in Table-4.

$$q_e = \frac{Q_0 K_L C_e}{1 + K_L C_e} \qquad (4)$$

where, q_e (mg/g) is the amount adsorbed; Q_0 (mg/g)is the saturated adsorption amount; K_L (L/mg)is the adsorption equilibrium constant of Langmuir isotherm; and C_e (mg/L)is the adsorption equilibrium concentration. The amount of NR adsorbed, q_e (mg/g) was calculated by $q_e = (C_o - C_e) \times (V/m)$, where, C_o (mg/L) is the initial concentration of the NR in solution, V (L) the volume of solution and m (g) is the mass of samples.

$$q_e = K_F C_e^{\frac{1}{n}} \qquad (5)$$

where K_F, (L/mg) is the empirical constant of Freundlich isotherm; the constant n is the empirical parameter related to the intensity of adsorption. When 1/n values are in the range of 0.1−1, the adsorption process is favorable.

Compared with Freundlich isotherm model, the Langmuir isotherm model yielded a higher correlation coefficient, that more than 0.99. Consequently, the Langmuir isotherm fitted the experimental data well, which illustrated that the adsorption mechanism was involved in this NR adsorption process, the surface adsorption sites and sorption energies of adsorbent was homogenous in its distribution.

The adsorption isothermal curve of NR on SGC is shown in Fig. 8. Table-4 showed the parameters obtained for NR from the Langmuir isotherm Q_0 and K_L were 136.98 mg/g, 0.5703 L/mg for SGC. The hydrophobic interaction of the adsorbent surface is one of the important determinants of adsorption capacity because water molecules can compete with the adsorbate at the adsorption sites [15]. When water is used as the solvent, the low hydrophobicity of the surface reduces the adsorption capacity of the adsorbent [16]. Therefore, the surface polarity of SGC is low, making this material more hydrophobic. The strong hydrophobic of the SGC surface might explain the high adsorption capacity for NR. The surface area of the microspore on SGC (273 m^2/g) was two–thirds than that of BET surface area of SGC (422 m^2/g). The result from NR adsorption capacity of SGC, demonstrate that hydrophobicity interaction may have played a key role in the NR adsorption.

The adsorption capacity of SGC is compared with various adsorbents in the literature [2, 15–19] as shown in Table-5. The results from our study were found to be higher than that of some adsorbents such as Fe_3O_4 hollow nanospheres (105 mg/g), peanut hull (87.72 mg/g), halloysite nanotubes (54.85 mg/g), and peanut husk (37.46 mg/g).
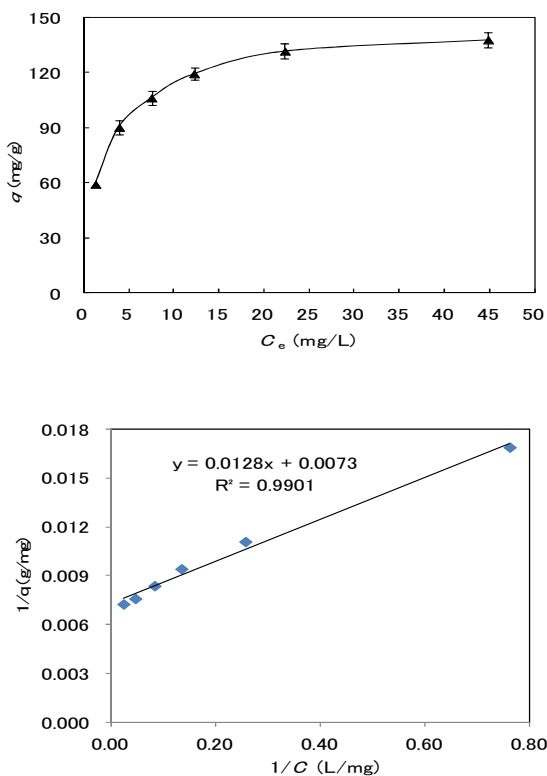
Fig. 8: Adsorption isothermal curve of NR on the SGC (C_o =25 to 100 mg/L, shaking time 2 h, adsorbent dose=0.4 g/L, at pH 5.0 and 25 °C).

Table-4: Parameters of adsorption isotherms of NR on SGC at 25 °C

Model	Constants
Langmuir isotherm	
Q_0 (mg/g)	136.98
K_L(L/mg)	0.5703
R^2	0.9901
Freundlich isotherm	
K_F (L/mg)	8.2883
n	4.1528
R^2	0.9331

Table-5: Maximum uptake capacity for the adsorption of NR onto various adsorbents

Adsorbents	Uptake capacity (mg/g)	References
Mn–impregnated activated carbons prepared from Typha orientalis	198.32	[15]
Spent cottonseed hull substrate	166.70	[16]
Spent ground coffee	136.98	This study
Fe₃O₄ hollow nanospheres	105.00	[17]
Peanut hull	87.72	[2]
Halloysite nanotubes	54.85	[18]
Peanut husk	37.46	[19]

Thermodynamic Analyses

Thermodynamic parameters are the actual indicators for the practical application process. Generally, ΔG^o is the standard free energy change (kJ/mol), $\Delta H°$ is the standard enthalpy (kJ/mol), $\Delta S°$ is the standard entropy (J/mol k), which was used to speculate on the adsorption mechanism. These thermodynamic parameters are determined using the following equations:

$$\Delta G^o = -RT \text{Ln} \frac{C_{ad.e}}{C_e} \tag{6}$$

$$\text{Ln} \frac{C_{ad.e}}{C_e} = \frac{\Delta S^o}{R} - \frac{\Delta H^o}{R}\frac{1}{T} \tag{7}$$

where, R is the universal gas constant (8.314 J/mol K); T is the temperature in Kelvin. $C_{ad,e}$ and C_e are correspond to the equilibrium concentrations of NB (mg/L) on the adsorbent and the solution, respectively. The values of $\Delta H°$ and $\Delta S°$ are determined from the slope and intercept,

Respectively, of van' Hoff plot ($\text{Ln} \frac{C_{ad.e}}{C_e}$ versus 1/T).

Table-6 displays the values of ΔG^o, which was calculated from −6.79 to−6.14 kJ/mol for SCG. It was noted that the ΔG^o values were all negative, which indicated these process the feasibility and spontaneous. The positive value of $\Delta H°$ (0.22 kJ/mol) suggests that the adsorption process is endothermic in nature. The positive value of $\Delta S°$ (20.54 J/mol k) indicated the affinity of the adsorbents for removal of NR as a result of the increased randomness at the interface among the solid liquid phases [18].

Table-6: Thermodynamic parameters for Adsorption NR on SGC

T (K)	ΔG^o (kJ/mol)	$\Delta H°$ (kJ/mol)	$\Delta S°$ (J/mol k)
283	−6.14		
298	−6.47	0.22	20.54
313	−6.79		

Conclusion

The removal ratio of NR is increased with increasing the pH value. The removal

ratios of NR (25 and 40 mg/L) on SGC after 2 h were 95.6 and 90.2%, respectively. Equilibrium data fitted very well in a Langmuir isotherm equation, the adsorption capacity of NR was 136.98 mg/g for SGC. The adsorption mechanisms can contributed to hydrophobicity interaction at the interface occurs between NR and SGC. The result from our study shows that the spent ground coffee can be used as effective adsorbent for the removal of neutral red from aqueous solutions.

Acknowledgments

References

1. Y. Bulut and H. A. Aydin, Kinetics and Thermodynamics Study of Methylene Blue Adsorption on Wheat Shells, *Desalination,* **194,** 259 (2006).
2. R. Gong, M. Li, C. Yang, Y. Sun and J. Chen, Removal of Cationic Dyes from Aqueous Solution by Adsorption on Peanut Hull, *J. Hazard. Mater.,* **B 121**, 247 (2005).
3. M. Dogan, H. Abak and M. Alkan, Biosorption of Methylene Blue from Aqueous Solutions by Hazelnut Shells: Equilibrium, Parameters and Isotherms, *Water Air Soil Pollut.,* **192**, 141 (2008).
4. L. S. Oliveira, A. S. Franca, T. M. Alves and S. D. F. Rocha, Evaluation of Untreated Coffee Husks as Potential Biosorbents for Treatment of Dye Contaminated Waters, *J. Hazard. Mater.,* **155**, 507 (2008).
5. G. Annadurai, R. Juang and D. Lee: Use of Cellulose–Based Wastes for Adsorption of Dyes from Aqueous Solutions, *J. Hazard. Mater.,* **B 92**, 263 (2002).
6. G. Mckay, G. Ramprasad and P. Pratapamowli, Equilibrium Studies for the Adsorption of Dyestuffs from Aqueous Solution by Low–Cost Materials, *Water Air Soil Pollut.,* **29**, 273 (1986).
7. F. Banat, S. Al–Asheh, R. Al–Ahmad and F. Bni–Khalid, Bench–Scale and Packed Bed Sorption of Methylene Blue Using Treated Olive Pomace and Charcoal. Bioresour Technol, **98**, 3017 (2007).
8. E. E. Kwon, H. Yi and Y. J. Jeon, Sequential Co-Production of Biodiesel and Bioethanol with Spent Coffee Grounds, *Bioresource Technol.,* **136**, 475 (2013).
9. A. S. Franca, L. S. Oliveira and M. E. Ferreira, Kinetics and Equilibrium Studies of Methylene Blue Adsorption by Spent Coffee Grounds, *Desalination,* **249**, 267 (2009).
10. C. Bouchelta, M. S. Medjram, O. Bertr and J. P. Bellta, Preparation and Characterization of Activated Carbon from Date Stones by Physical Activation with Steam, *J. Anal. Appl. Pyrolysis.,* **82**, 70 (2008).
11. J. H. D. Boer, B. G. Linsen, T. V. D. Plas and G. J. Zondervan, Studies on Pore Systems in CatalystsVII. Description of the Pore Dimensions of Carbon Blacks by the t Method, *J. Cataly,* **4**, 649 (1965).
12. J. P. Olivier, Modelling Physical Adsorption on Porous and Nonporous Solids Using Density Functional Theory, *J. Porous. Mater.,* **2**, 9 (1995).
13. H. P. Boehm, Surface Oxides on Carbon and their Analysis: a Critical Assessment. *Carbon,* **40**, 145 (2002).
14. Y. S. Al–Degs, M. I. Ei-Barghouthi, A. H. El-Sheikh and G. M. Walker, Effect of Solution pH, Ionic Strength, and Temperature on Adsorption Behavior of Reactive Dyes on Activated Carbon, *Dyes Pigments.,* **77**, 16 (2008).
15. J. Zhang, Q. Shi, C. Zhang, J. Xu, B. Zhai and B. Zhang, Adsorption of Neutral Red onto Mn-impregnated Activated Carbons Prepared from Typha Orientalis, *Bioresource Technol.,* **99**, 8974 (2008).
16. Q. Zhou, W. Gong, C. Xie, D. Yang, X. Ling, X. Yuan, S. Chen and X. Liu, Removal of Neutral Red from Aqueous Solution by Adsorption on Spent Cottonseed Hull Substrate, *J. Hazard. Mater.,* **185**, 502 (2011).
17. M. Irama, C. Guo, Y. Guan, A. Ishfag and H. Liu, Adsorption and Magnetic Removal of Neutral Red Dye from Aqueous Solution Using Fe_3O_4 Hollow Nanospheres, *J. Hazard. Mater.,* **181**, 1039 (2010).
18. P. Luo, Y. Zhao, B. Zhang, J. Liu, Y. Yang and J. Liu: Study on the Adsorption of Neutral Red from Aqueous Solution onto Halloysite Nanotubes, *Water Res.,* **44**, 1489 (2010).
19. R. Han, P. Han, Z. Cai, Z. Zhao and M. Tang, Kinetics and Isotherms of Neutral Red Adsorption on Peanut Husk, *J. Environ. Sci.,* **20**, 1035 (2008).